Korean J. Chem. Eng., **26**(2), 523-527 (2009)

Syngas combustion characteristics of four oxygen carrier particles for chemical-looping combustion in a batch fluidized bed reactor

Ho-Jung Ryu*,†, Dowon Shun*, Dal-Hee Bae*, and Moon-Hee Park**

*Korea Institute of Energy Research, Daejeon 305-343, Korea
**Hoseo University, Asan 336-795, Korea
(*Received 6 June 2008 • accepted 29 September 2008*)

Abstract−Syngas combustion characteristics of oxygen carrier particles have been investigated. Experiments were performed on four oxygen carrier particles in a fluidized bed reactor. All four oxygen carrier particles showed high gas conversion, high CO_2 selectivity, and low CO concentration in the reducer and very low NOx (NO, NO_2, N_2O) emissions in the oxidizer. Moreover, all particles showed good regeneration ability during successive reduction-oxidation cyclic tests up to the 10^{th} cycle. The results indicate that inherent CO_2 separation, NOx-free combustion, and long-term operation without reactivity decay of oxygen carrier particles are possible in a syngas fueled chemical-looping combustion system with NiO/bentonite, NiO/$NiAl_2O_4$, Co_xO_y/$CoAl_2O_4$, and OCN-650 particles. However, Co_xO_y/$CoAl_2O_4$ represented slight decay of oxidation reactivity with the number of cycles increased and the oxidation rate slower than other particles.

Key words: Chemical-looping, Oxygen Carrier, Carbon Dioxide, Nitrogen Oxides, Syngas

INTRODUCTION

Carbon dioxide, a major greenhouse gas, is produced in large quantities from combustion of fossil fuels, much of this related to electric power generation. In a conventional power generation system, fuel and air are directly mixed and burned; therefore, it is not easy to separate CO_2 from flue gas because CO_2 is diluted by N_2 in air. Chemical-looping combustion (CLC) is a novel combustion technology with inherent separation of the greenhouse gas CO_2 and low NOx emission. The chemical-looping combustor consists of two reactors, an oxidation reactor and a reduction reactor, as shown in Fig. 1. Fuel and Air go through the different reactors. Eqs. (1) and (2) illustrate a basic concept of the chemical-looping combustion system. In the reduction reactor, gaseous fuel (CH_4, H_2, CO or C_nH_{2n+2}) reacts with metal oxide according to Eq. (2), and release water vapor and carbon dioxide from the top and metal particles (M) from the bottom. The solid products, metal particles, are transported to the oxidation reactor and react with oxygen in the air according to Eq. (1), and produce high-temperature flue gas and metal oxide particles. Metal oxide particles at high temperature are again introduced to the reduction reactor and supply the heat required for the reduction reaction. Between the two reactors, metal (or metal oxide) particles play an important role in transportation of oxygen and heat; therefore, the looping material between the two reactors is named as an oxygen carrier particle.

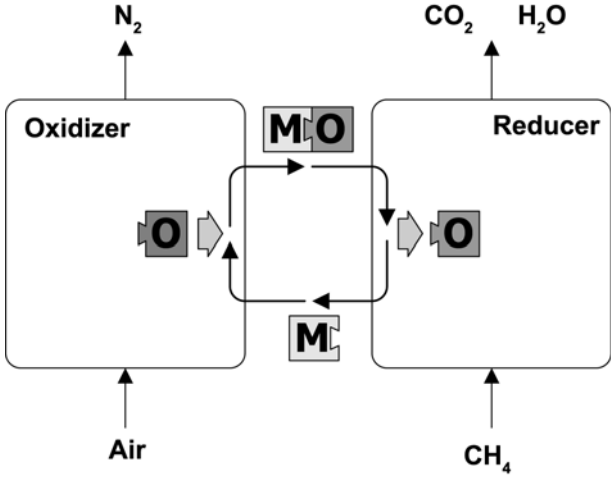

Fig. 1. Simplified schematic of chemical-looping combustion.

Oxidation: exothermic reaction,

$$M+0.5\ O_2=MO \quad (1)$$

Reduction: endothermic reaction,

$$CH_4+4MO=CO_2+2H_2O+4M \quad (2)$$

It is important for the exhaust gas from the reduction reactor to contain only highly concentrated CO_2 and water vapor. Therefore, CO_2 can be easily recovered by cooling the exhaust gas without any extra energy consumption (energy penalty) for CO_2 separation. Another advantage of CLC is that NOx formation can be thoroughly eliminated because the oxidation reaction occurs at a considerably lower temperature (~900 °C) without a flame; therefore, there is no thermal NOx formation [1,2]. Moreover, the efficiency of chemical-looping combustion system is very high. Wolf et al. [3] reported that a natural gas-fueled chemical-looping combustor achieves a thermal efficiency between 52-53% and is 5 percent points more efficient than an NGCC system with state-of-the-art technologies for CO_2 capture.

The previous results on chemical-looping combustion technology have concentrated on improvement of the oxygen carrier par-

†To whom correspondence should be addressed.
E-mail: hjryu@kier.re.kr

ticles and most of the studies used methane or hydrogen as a reduction gas [4]. To understand the performance and the feasibility of the chemical-looping combustion system, it is necessary to check the performance of the oxygen carrier particles by using gaseous fuel such as natural gas and syngas. Moreover, confirmation of reduction of NOx emission in the oxidizer and high CO_2 selectivity in the reducer is a prerequisite for application of the chemical-looping combustion system in commercial plants.

There are many reports on the reactivity of oxygen carriers for a chemical-looping combustor, but most of the previous works were performed with a TGA or fixed bed reactor and the data of gas concentrations from oxidizer and reducer were infrequent. Moreover, there is no report on NOx emissions during oxidation at all. Adanez et al. [5] used a TGA for reaction tests, and there are no data on gas concentration during reduction and oxidation. Corbella et al. [6] used a fixed bed reactor, but they measured gas concentration with a TPR. In their report, gas concentrations were plotted with an arbitrary unit and quantitative analyses of gas conversion and CO_2 selectivity were not provided. Diego et al. [7] used a fluidized bed reactor, and they reported the product gas distribution, but the effect of the number of cycles on the product gas distribution was provided only for CO_2 concentration. Moreover, Diego et al. [7] did not measure the NOx concentration during oxidation. Recently, Ryu et al. [8] reported natural gas combustion characteristics of three oxygen carriers in a fluidized bed reactor. In their report, CO_2 selectivity, NOx concentration data were provided.

Natural gas has been considered as a major fuel in the chemical-looping combustor so far. However, syngas has lately attracted considerable attention as a fuel that can substitute for natural gas in the chemical-looping combustor because of high oil prices. However, there is a lack of experimental data on syngas-fueled chemical-looping combustion. Mattison et al. [9] used a TGA and a batch fluidized bed for syngas combustion tests, but the effect of temperature on the product gas distribution was provided only for CO concentration. Johansson et al. [10] used a fluidized bed reactor for syngas combustion tests, and they reported the product gas distribution, but did not measure the NOx concentration during oxidation.

In this study, syngas combustion characteristics of oxygen carrier particles were investigated in a batch type fluidized bed reactor (0.05 m ID, 0.7 m high). Four particles, NiO/bentonite, NiO/$NiAl_2O_4$, $Co_xO_y/CoAl_2O_4$, OCN-650, were used as oxygen carrier particles. Simulated syngas and air were used as reactants for reduction and oxidation, respectively. To check feasibility of good performance, inherent CO_2 separation, and low-NOx emissions, CH_4, CO, CO_2, O_2, H_2, NO, NO_2, N_2O concentrations were measured by on-line gas analyzer. Moreover, the regeneration ability of the oxygen carrier particles was investigated by successive reduction-oxidation cyclic tests up to the 10^{th} cycle.

EXPERIMENTAL SECTION

Multi-cycle tests were carried out in a bubbling fluidized bed reactor. A schematic of the reactor is shown in Fig. 2. The major components consist of a gas input system, the fluidization column, a hot gas filter, a condenser, a gas cooler, and a gas sampling/analyzing unit. The fluidization column is 0.7 m high with an internal diameter of 0.05 m. A perforated gas distributor plate separates the

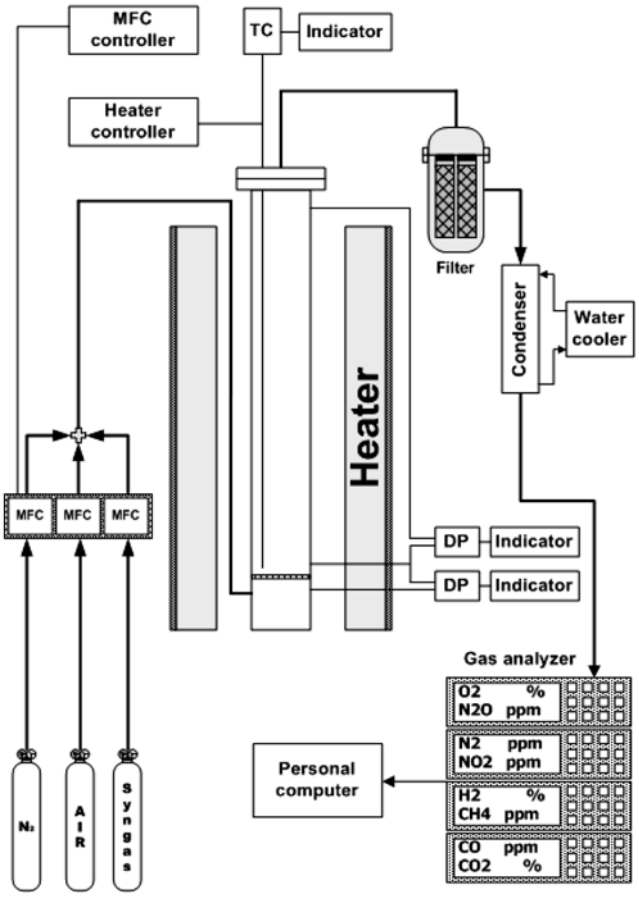

Fig. 2. Schematic of bubbling fluidized bed reactor.

fluidization column and the air box. Reactant gas was fed to the air box. An electric heater could be controlled by a thermocouple and a heater controller. Thermocouple measurements of temperature and pressure transducer data were recorded by a data acquisition system. The exit stream from the fluidized bed reactor was sampled at the outlet of the reactor. The CH_4, CO, CO_2, H_2, NO, NO_2, N_2O, and O_2 concentrations were determined by an on-line gas analyzer and recorded by the data acquisition system. Further details of the reactor system are available elsewhere [11].

The four oxygen carrier particles tested were NiO/bentonite, NiO/$NiAl_2O_4$, $Co_xO_y/CoAl_2O_4$, and OCN-650. For economical operation of the chemical-looping combustor, the cost of the oxygen carrier is a very important factor. However, most of the previous researchers used oxygen carriers made of expensive chemical-grade raw materials that produced only a small amount of carriers for tests in the TGA, fixed bed, and small scale fluidized bed. If we want to operate a larger plant to demonstrate continuous long-term operation of the chemical-looping combustor, mass production of carriers is prerequisite and cheaper raw materials will be helpful to save make-up costs of carriers and operating costs of the chemical-looping combustor. In this study, NiO/bentonite particles were made of commercial-grade raw materials. The cost of raw materials is less than 65% of other carriers. We also used NiO/$NiAl_2O_3$ and $Co_xO_y/CoAl_2O_4$ particles made of chemical-grade raw materials for comparison with NiO/bentonite particles. Moreover, OCN-650 particles

were produced by spray-drying method and have spherical shape.

In our previous works [11-16], many kinds of oxygen carrier particles such as NiO/bentonite, NiO/$NiAl_2O_3$, $Co_xO_y/CoAl_2O_4$, (NiO+Fe)/bentonite, NiO/YSZ, (NiO+Fe)/YSZ, NiO/hexaaluminate, Co_xO_y/hexaaluminate, OCN-650 were developed and reactivity and attrition resistance of carriers were tested by using TGA, fluidized bed and ASTM attrition tester (D5757-95). Based on the previous results, we selected those four carriers as candidates.

Prior to the start of each experiment, the oxygen carrier particle was sieved to ensure that all particles were initially between 106 and 212 μm in size. The static bed height was 0.4 m in all cases, and the experiments were carried out batchwise for the particles, i.e., no particles were added during the run. The fluidized bed reactor operated with a total inlet gas flow of 2.0 N*l*/min in all cases, corresponding to superficial gas velocities of 0.07 m/s at 900 °C. Particles were oxidized in air as the bed temperature was increased from room temperature to 900 °C. Once the particle was fully oxidized, the particle was exposed to a gas mixture. The gas mixture contained 45% syngas and 55% N_2 for all reduction tests. The inlet concentrations were measured by bypassing the reactor. In this study, we selected the composition of the simulated syngas as H_2 : CO_2 : CO=30 : 10 : 60, to simulate syngas from a coal gasifier of Shell and Texaco (Shell: H_2 : CO_2 : CO=31.6 : 0.8 : 64.0; Texaco: H_2 : CO_2 : CO=27.8 : 12.5 : 40.0) [17]. Between the cyclic oxidation and reduction tests, nitrogen was used as a purge gas. A rapid decrease in the exit gas concentration marked the end of purge. For each particle, ten cycles of reduction–oxidation were carried out. The properties and preparation methods of four oxygen carriers and experimental conditions are summarized in Tables 1 and 2, respectively.

Table 2. Summary of experimental conditions

Variables \ Particles	NiO/bentonite, NiO/$NiAl_2O_4$, Co_xO_y/$CoAl_2O_4$, OCN-650
Static bed height [m]	0.4
Temperature [°C]	900, Isothermal
Method	(Red./Pur./Oxi./Pur.=10/10/30/10 min) ×10 cycles
Purge gas	N_2 (2.0 *l*/min)
Reactant gas (reduction)	Simulated syngas (0.89 *l*/min) +N_2 (1.11 *l*/min)
Reactant gas (oxidation)	Air (2.0 *l*/min)

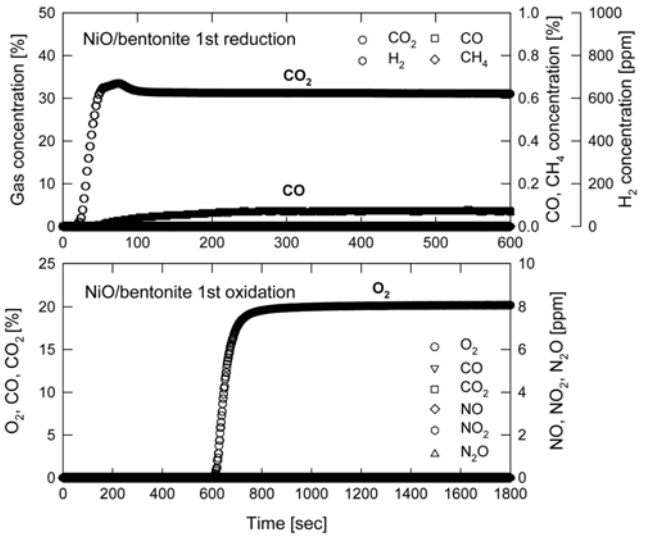

Fig. 3. Typical trends of gas concentrations during the first reduction and oxidation cycle.

RESULTS AND DISCUSSION

Typical traces of gas concentration versus time for the NiO/bentonite particles during the reduction and the oxidation for the first cycle appear in Fig. 3. The ordinate of this figure is dry-based concentration. At the beginning of the reduction, CO_2 concentration increased, and then reached a constant value. The CO_2 concentration was 31-33% because of dilution by nitrogen. During the reduction, the average concentration of CO was 0.03% and CH_4 was 0%. Moreover, the average selectivity of carbon in the consumed fuel to CO_2 was 99.3%. The results indicate that most of CO and H_2 in the syngas react with oxygen in the particles and produce only CO_2 and water vapor.

At the beginning of the oxidation, oxygen was not detected. After some time, the O_2 concentration increased quickly, and then maintained constant at 21%. During the oxidation, NO, NO_2, and N_2O were not detected at all. The deposited carbon during reduction can be detected by measuring CO and CO_2 concentration during oxidation because it will be burnt by oxygen in the air during oxidation. As shown in Fig. 3, CO and CO_2 were not detected at all during oxidation.

The effects of reduction-oxidation cycling on the fuel conversion of four oxygen carrier particles during reduction are shown in Fig. 4. The fuel conversion is defined as (moles of reacted fuel)/(moles of input fuel). The moles of reacted fuel are calculated by measured CO and CO_2 concentration. The input fuel concentration was measured before each cycle by bypassing the reactor. The fuel conversions for NiO/bentonite, NiO/$NiAl_2O_4$ and OCN-650 particles increased slightly with the number of cycles. We assumed that the internal pore structure can be changed during successive reduction and oxidation cycles at 900 °C. We measured the porosity of fresh carriers and particles after the 10th cycle test by mercury po-

Table 1. Properties and preparation methods of four oxygen carrier particles

Oxygen carrier particles	NiO/bentonite	NiO/$NiAl_2O_4$	Co_xO_y/$CoAl_2O_4$	OCN-650
Particle size range [μm]	106-212	106-212	106-212	106-212
Metal oxide wt%	60	70	70	60
Bulk density [kg/m^3]	1172	1520	1024	903
Preparation methods	Mixing	Dissolution	Coprecipitation & Impregnation	Spray drying

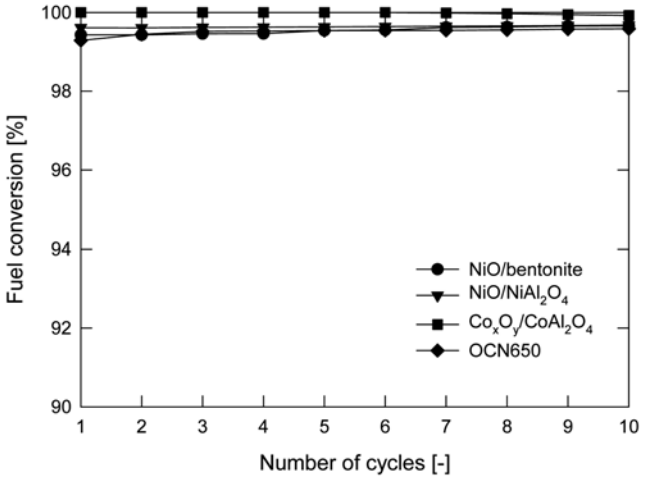

Fig. 4. Fuel conversion vs. number of cycles.

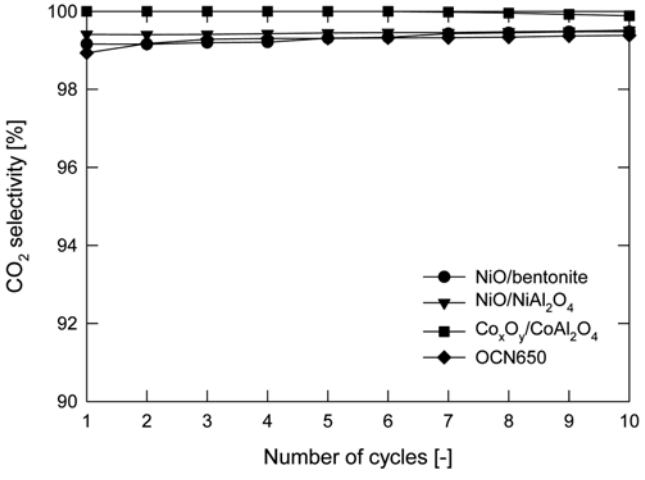

Fig. 5. CO_2 selectivity vs. number of cycles.

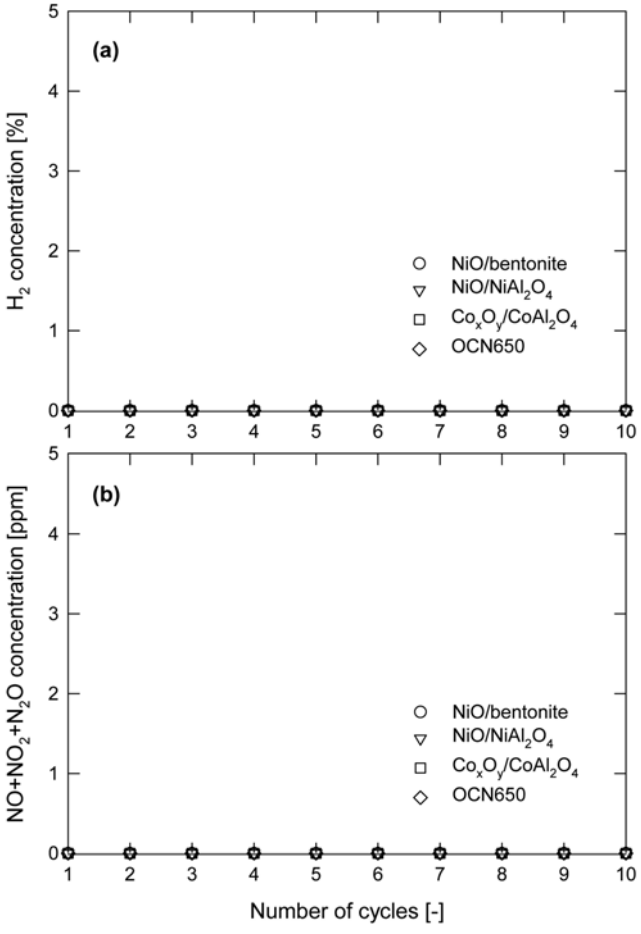

Fig. 6. (a) H_2 concentration vs. number of cycles and (b) NOx concentration vs. number of cycles.

rosimeter. The porosity of those three particles after the 10th cycle was slightly higher than that of fresh particles, but the porosity of $Co_xO_y/CoAl_2O_4$ particle decreased after cyclic test. The average values of fuel conversion during ten cycles for NiO/bentonite, NiO/$NiAl_2O_4$, $Co_xO_y/CoAl_2O_4$, and OCN-650 particles were very high, the values being 99.5, 99.6, 100, 99.3%, respectively.

The effects of reduction-oxidation cycling on the CO_2 selectivity of four oxygen carrier particles during reduction are shown in Fig. 5. CO_2 selectivity indicates the portion of CO_2 per carbon in consumed fuel ([CO_2]/[Carbon in consumed fuel]). The CO_2 selectivity for NiO/bentonite, NiO/$NiAl_2O_4$, and OCN-650 particles slightly increased with the number of cycles, consistent with Fig. 4. The average values of CO_2 selectivity during ten cycles for NiO/bentonite, NiO/$NiAl_2O_4$, $Co_xO_y/CoAl_2O_4$, and OCN-650 particles were very high and the values were 99.3, 99.4, 100, 98.9%, respectively.

Fig. 6(a) and (b) represent hydrogen concentration during reduction and NOx concentration during oxidation, respectively. Hydrogen was not detected at all for all four particles, as shown in Fig. 6(a). This result indicates that all of the hydrogen in the syngas was converted to water. Moreover, NO, NO_2, and N_2O were not detected for all cycles and for all particles, as shown in Fig. 6(b). Based on the results, we could conclude that NOx-free combustion is realizable in the syngas fueled chemical-looping combustion system with NiO/bentonite, NiO/$NiAl_2O_4$, $Co_xO_y/CoAl_2O_4$, and OCN-650 particles.

Fig. 7 shows the O_2 concentration profile during successive oxidation reaction up to the 10^{th} cycle. All four particles represented good regeneration ability during oxidation. However, $Co_xO_y/CoAl_2O_4$ particle showed slight decay of oxidation reactivity as the number of cycles increased and oxidation rates (slope of breakthrough curve) were slower than other particles. These results indicate that the $Co_xO_y/CoAl_2O_4$ particle can cause some problems during long-term operation.

CONCLUSIONS

Syngas combustion characteristics of oxygen carrier particles were investigated in a batch type bubbling fluidized bed reactor (0.05 m ID, 0.7 m high). Four particles, NiO/bentonite, NiO/$NiAl_2O_4$, $Co_xO_y/CoAl_2O_4$, OCN-650, were used as oxygen carrier particles. Simulated syngas and air were used as reactants for reduction and oxidation, respectively. To check feasibility of good performance, inherent CO_2 separation, and low-NOx emissions, CH_4, CO, CO_2, O_2, H_2, NO, NO_2, N_2O concentrations were measured by on-line gas analyzer. Moreover, the regeneration ability of the oxygen carrier

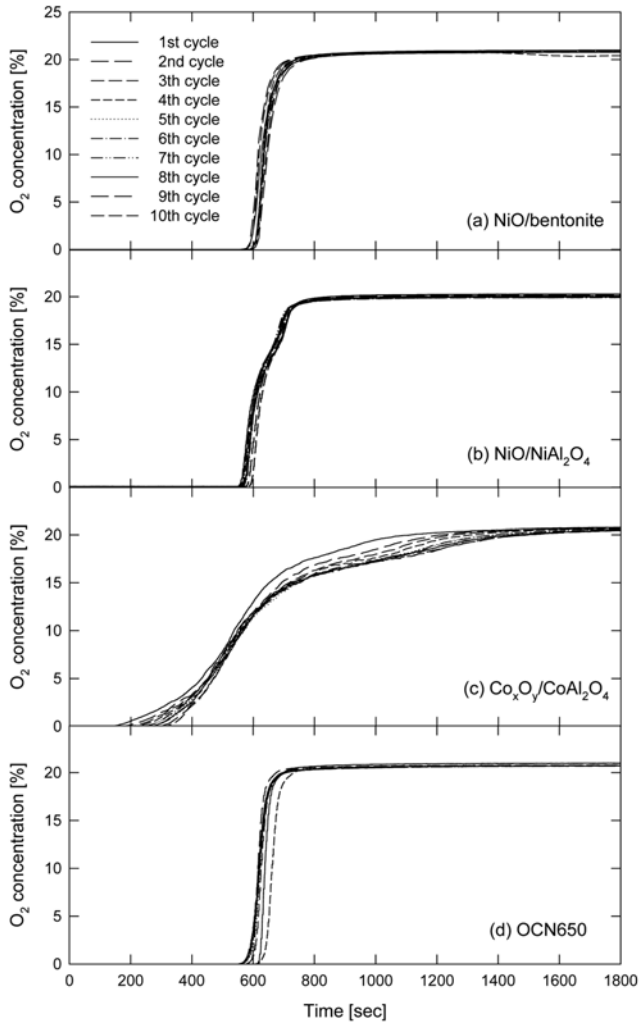

Fig. 7. O_2 concetration profiles during successive oxidation cycles.

particles was investigated by successive reduction-oxidation cyclic tests up to the 10^{th} cycle. All four oxygen carrier particles showed high gas conversion, high CO_2 selectivity, and low CO concentration during reduction and no NOx (NO, NO_2, N_2O) emissions during oxidation. All four particles showed good regeneration ability during successive reduction-oxidation cyclic tests up to the 10^{th} cycle. These results indicate that inherent CO_2 separation, NOx-free combustion, and long-term operation without reactivity decay of oxygen carrier particles are possible in the syngas fueled chemical-looping combustion system with NiO/bentonite, $Ni/NiAl_2O_4$, $Co_xO_y/CoAl_2O_4$ and OCN-650 particles. However, $Co_xO_y/CoAl_2O_4$ represented slight decay of oxidation reactivity with the number of cycles increased, and the oxidation rate was slower than other particles.

ACKNOWLEDGMENT

This work was supported by Ministry of Knowledge Economy (MKE) through Electric Power Industry Technology Evaluation & Planning Center (ETEP).

REFERENCES

1. M. Ishida and H. Jin, *Energy Convers. Mgmt.*, **38**, S187 (1996).
2. H. Jin, T. Okamoto and M. Ishida, *Energy Fuels*, **12**, 1272 (1998).
3. J. Wolf, M. Anheden and J. Yan, *Fuel*, **84**, 993 (2005).
4. H. J. Ryu, *CO_2-NOx free chemical-looping combustion technology*, KOSEN 21 Advanced Technology Report, www.kosen21.org (2003).
5. J. Adánez, L. F. de Diego, F. García, P. Gayán and A. Abad, *Energy Fuels*, **18**, 371 (2004).
6. B. M. Corbella, L. F. de Diego, F. García, J. Adánez and J. M. Palacios, *Energy Fuels*, **19**, 433 (2005).
7. L. F. Diego, P. Gayán, F. García, J. Celaya, A. Abad and J. Adánez, *Energy Fuels*, **19**, 1850 (2005)
8. H. J. Ryu, G. T. Jin, S. H. Jo and M. H. Park, *Chem. Eng. Japan*, accepted (2008).
9. T. Mattisson, F. Garcia-Labiano, B. Kronberger, A. Lyngfelt, J. Adanez and H. Hofbauer, *Int. J. of Greenhouse Gas Control*, **1**, 158 (2007).
10. E. Johansson, T. Mattisson, A. Lyngfelt and H. Thunman, *Chemical Engineering Research and Design*, **84**, 819 (2006).
11. H. J. Ryu, D. H. Bae and G. T. Jin, *in 31st KOSCO Symposium*, 141 (2005).
12. H. J. Ryu, D. H. Bae, K. H. Han, S. Y. Lee, G. T. Jin and J. H. Choi, *Korean J. Chem. Eng.*, **18**, 831 (2001).
13. H. J. Ryu, D. H. Bae and G. T. Jin, *Korean J. Chem. Eng.*, **20**, 960 (2003).
14. H. J. Ryu, G. T. Jin, N. Y. Lim and S. Y. Bae, *Trans. Korean Hydrogen Energy Society*, **14**, 24 (2003).
15. H. J. Ryu, D. H. Bae, S. H. Jo and G. T. Jin, *Korean Chem. Eng. Res.*, **42**, 107 (2004).
16. H. J. Ryu, J. W. Kim, W. K. Jo and M. H. Park, *Korean Chem. Eng. Res.*, **45**, 506 (2007).
17. G. B. Han, N. K. Park, S. O. Ryu and T. J. Lee, *Korean Chem. Eng. Res.*, **44**, 356 (2006).